

1 **Brunner syndrome associated MAOA dysfunction in human dopaminergic neurons**
2 **results in NMDAR hyperfunction and increased network activity.**

3 **Running title: MAOA deficiency leads to increased neuronal activity**

4 Yan Shi^{1*}, Jon-Ruben van Rhijn^{2*}, Maren Bormann², Britt Mossink^{1,2}, Monica Frega^{1,3},
5 Hatice Recaioglu¹, Marina Hakobjan¹, Teun Klein Gunnewiek^{1,4}, Chantal Schoenmaker¹,
6 Elizabeth Palmer^{5,6}, Laurence Faivre^{7,8}, Sarah Kittel-Schneider^{9,10}, Dirk Schubert², Han
7 Brunner^{1,12}, Barbara Franke^{1,11#}, Nael Nadif Kasri^{1,2#}

8 *These authors contributed equally

9 #Shared final responsibility

10 ¹Department of Human Genetics, Donders Institute for Brain, Cognition and Behavior,
11 Radboud University Medical Center, Nijmegen, The Netherlands

12 ²Department of Cognitive Neuroscience, Donders Institute for Brain, Cognition and
13 Behavior, Radboud University Medical Center, Nijmegen, The Netherlands

14 ³Department of Clinical neurophysiology, University of Twente, 7522, NB Enschede,
15 Netherlands

16 ⁴Department of Anatomy, Donders Institute for Brain, Cognition and Behavior, Radboud
17 University Medical Center, Nijmegen, The Netherlands

18 ⁵Genetics of Learning Disability Service, Hunter Genetics, Waratah, NSW, Australia

19 ⁶School of Women's and Children's Health, University of New South Wales, Randwick,
20 NSW, Australia

21 ⁷Centre de Référence Anomalies du développement et Syndromes malformatifs and FHU
22 TRANSLAD, Hôpital d'Enfants, Dijon, France

23 ⁸INSERM UMR1231 GAD, Faculté de Médecine, Université de Bourgogne, Dijon, France.

24 ⁹Department of Psychiatry, Psychosomatic Medicine and Psychotherapy, University Hospital,
25 Goethe-University, Frankfurt, Germany

26 ¹⁰Department of Psychiatry, Psychosomatic Medicine and Psychotherapy, University
27 Hospital Würzburg, Würzburg, Germany

28 ¹¹Department of Psychiatry, Donders Institute for Brain, Cognition and Behavior, Radboud
29 University Medical Center, Nijmegen, The Netherlands

30 ¹² Department of Clinical Genetics, MUMC+, GROW School of Oncology and
31 Developmental Biology, and MHeNS School of Neuroscience and Maastricht University,
32 Maastricht, the Netherlands

33

34 Corresponding author: Nael Nadif Kasri; Radboud University Medical Centre, Department of
35 Human Genetics, Geert Grooteplein 10, 6525GA, Nijmegen, The Netherlands. Tel: +31 24
36 3614242, e-mail: Nael.NadifKasri@radboudumc.nl

37 Key words: Brunner syndrome, MAOA, human iPSC, Dopaminergic neuron, NMDA
38 receptor, microelectrode array

39 **Abstract**

40 **Background:** Monoamine neurotransmitter abundance affects motor control, emotion, and
41 cognitive function and is regulated by monoamine oxidases. Amongst these, monoamine
42 oxidase A (MAOA) catalyzes the degradation of dopamine, norepinephrine, and serotonin into
43 their inactive metabolites. Loss-of-function mutations in the X-linked *MAOA* gene cause
44 Brunner syndrome, which is characterized by various forms of impulsivity, maladaptive
45 externalizing behavior, and mild intellectual disability. Impaired MAOA activity in individuals
46 with Brunner syndrome results in bioamine aberration, but it is currently unknown how this
47 affects neuronal function.

48 **Methods:** We generated human induced pluripotent stem cell (hiPSC)-derived dopaminergic
49 (DA) neurons from three individuals with Brunner syndrome carrying different mutations, and
50 used CRISPR/Cas9 mediated homologous recombination to rescue MAOA function. We used
51 these lines to characterize morphological and functional properties of DA neuronal cultures at
52 the single cell and neuronal network level *in vitro*.

53 **Results:** Brunner syndrome DA neurons showed reduced synaptic density but hyperactive
54 network activity. Intrinsic functional properties and α -amino-3-hydroxy-5-methyl-4-
55 isoxazolepropionic acid receptor (AMPA)-mediated synaptic transmission were not affected
56 by MAOA dysfunction. Instead, we show that the neuronal network hyperactivity is mediated
57 by upregulation of the *GRIN2A* and *GRIN2B* subunits of the N-methyl-D-aspartate receptor
58 (NMDAR), and rescue of *MAOA* results in normalization of NMDAR function as well as
59 restoration of network activity.

60 **Conclusions:** Our data suggest that MAOA dysfunction in Brunner syndrome increases
61 activity of dopaminergic neurons through upregulation of NMDAR function, which may
62 contribute to Brunner syndrome associated phenotypes.

63

64 **Introduction**

65 Dopamine, serotonin, and noradrenaline all belong to the class of monoamine
66 neurotransmitters. They are prevalent throughout the brain, and their abundance influences
67 brain development, function and behavior(1, 2). Monoamine neurotransmitter related activity
68 is tightly regulated, and dysregulation of monoaminergic pathways is associated with several
69 neuropsychiatric disorders including schizophrenia, major depressive disorder, autism
70 spectrum disorder (ASD), and attention deficit/hyperactivity disorder (ADHD). Monoamine
71 oxidases (MAOs) catabolize monoaminergic neurotransmitters(3) and thereby regulate the
72 monoamine concentration in the brain. Disruption of MAO activity can have profound
73 consequences on normal brain function(4). One disorder in which MAO function is strongly
74 affected is Brunner syndrome, a neurodevelopmental disorder characterized by hemizygous
75 mutations in the X-linked monoamine oxidase-A (*MAOA*) gene. Brunner syndrome was first
76 described in large Dutch kindred with non-dysmorphic borderline intellectual disability (ID),
77 and prominent impulsivity and maladaptive externalizing behavior(5, 6). More recently, three
78 more families have been reported with Brunner syndrome, strengthening the link between
79 MAOA dysfunction and Brunner syndrome. In all families, individuals carry either nonsense
80 or missense mutations of *MAOA*(7, 8).

81 The monoaminergic system has been associated with regulation of aggressive behavior, both
82 in wildtype animal models(9-12) and genetic models of neurodevelopmental disorders(13, 14).
83 For example, hemizygous *Maoa* mutant mice show abnormally high levels of aggressive
84 behavior and disturbed monoamine metabolism(15-17). Furthermore, *Maoa*-deficient mice
85 display alterations in brain development, with aberrant organization of the primary

86 somatosensory cortex(15) and increased dendritic arborization of pyramidal neurons in the
87 orbitofrontal cortex(17). Postnatal reduction of serotonin levels in *Maoa*-deficient mice
88 partially corrected some of these developmental abnormalities in the cortex(18). On the
89 molecular level, *Maoa* has been implicated in the regulation of synaptic neurotransmitter
90 receptors, as *Maoa* knockout mice show increased N-methyl-D-aspartate (NMDA) receptor
91 subunit expression in the prefrontal cortex(19). Taken together, these data suggest that
92 dysfunction of MAOA in rodents leads to both structural and functional alterations during brain
93 development.

94 MAOA is expressed in different neuronal as well as glial cell types in the brain(20). This
95 complex interplay of multiple monoaminergic pathways in brain function creates a challenge
96 in disentangling the cell-type specific roles of MAOA during neurodevelopment and in the
97 regulation of normal brain activity. So far, particular emphasis has been given to the
98 serotonergic system in MAOA research(21), as MAOA dysfunction results in increased
99 serotonin levels in both humans and mice(5, 7, 8, 15, 17, 22). Indeed, dysfunction of the
100 serotonergic system is associated with increased aggression and impulsivity(23). However, the
101 expression pattern of MAOA suggests it is primarily expressed in catecholaminergic
102 (dopaminergic and noradrenergic) neurons(21, 24), whereas expression in serotonergic
103 neurons is variable and decreases during development in the mouse brain(25). Abundant
104 expression of MAOA in dopaminergic (DA) neurons(24, 26) coincides with the finding that
105 changes in dopaminergic neuronal activity also directly affect impulsive and aggressive
106 behavior(27, 28).

107 Current advances in the generation of human induced pluripotent stem cell (hiPSC) induced
108 neurons enable us to generate cultures of defined cell types, which provides us opportunities to

109 disentangle the complexities that underlie interactions of multiple monoaminergic pathways.
110 We generated hiPSC-derived DA neurons from healthy individuals and individuals with
111 Brunner syndrome carrying missense or nonsense mutations to investigate the cellular and
112 molecular mechanisms underlying MAOA dysfunction in a homogenous human DA neuronal
113 network. Combining data on morphological analysis, gene expression, single-cell
114 electrophysiology, and neuronal network activity using microelectrode arrays (MEAs), we
115 show that increased network activity in MAOA-deficient DA neuronal networks is associated
116 with increased expression of the N-Methyl-D-Aspartate receptor (NMDAR) subunits *GRIN2A*
117 and *GRIN2B* and increased NMDAR function. Rescue of a *MAOA* missense mutation by
118 CRISPR/Cas9 resulted in restoration of *GRIN2A* and *GRIN2B* expression, NMDAR function,
119 and neuronal network activity to control values. Taken together, this work suggests that
120 increased network activity in DA neurons from individuals with Brunner syndrome is causally
121 linked to NMDAR hyperfunction.

122

123

124 **Methods and Materials**

125 Methods and materials are described in greater detail in the Supplemental Methods and
126 Materials.

127 **Cell Culture of hiPSCs and neuron differentiation**

128 Control hiPSC lines were derived from dermal fibroblasts of male healthy volunteers(29)(30).
129 The hiPSC lines ME2, ME8 and NE8 were derived from dermal fibroblast biopsies of male
130 individuals diagnosed with Brunner syndrome described previously(5-8). Ethical approval for
131 the study was obtained for all sites separately by local ethics committees. Written informed
132 consent was given by the parents or legal representatives of the participants. All hiPSC
133 reprogramming and characterization of the pluripotency markers was done by the Radboudumc
134 Stem Cell Technology Center (SCTC) (**Supplementary Figure 1**). The hiPSCs colonies were
135 split into single cells, and differentiated to a DA neuron identity using small molecules(31).
136 Rat astrocytes (prepared as previously described(32)) were cocultured with DA neuron
137 progenitors to promote maturation.

138 **Gene expression analysis and immunocytochemistry**

139 RNA was isolated with the RNeasy Mini Kit (Qiagen) and retro-transcribed into cDNA by
140 iScript cDNA Synthesis Kit (Bio-Rad Laboratories, Inc) according to the manufacturer's
141 instructions. We measured gene expression profiles using quantitative real-time PCR (qRT-
142 PCR). Primers are listed in **Supplementary Table S1**. DA neurons plated on glass coverslips
143 were used for immunocytochemistry and imaged using a Zeiss AxioImager Z1 with apotome
144 (Carl Zeiss AG, Germany). Synapse density was assessed through manual counting using Fiji
145 software.

146 **Neuronal reconstruction**

147 Widefield fluorescent images of MAP2-labelled hiPSC-derived DA neurons were
148 reconstructed using Neurolucida 360 (Version 2017.01.4, Microbrightfield Bioscience,
149 Williston, USA). All the morphological data were acquired and analyzed blind to the genetic
150 background of the neurons.

151 **MEA recording and Single-cell electrophysiology**

152 DA neuron progenitors (day *in vitro* 20, DIV20) were plated on 6-Well or 24-well MEA
153 devices (Multichannel Systems, MCS GmbH, Reutlingen, Germany). The neuronal network
154 activity of DIV73 DA neurons was measured and analyzed as described(32-34). Single-cell
155 electrophysiological recordings on coverslip containing DIV73 DA neurons were conducted
156 under continuous perfusion with oxygenated (95% O₂ / 5% CO₂) and heated (32°C) recording
157 artificial cerebrospinal fluid (ACSF).

158 **Statistical analysis**

159 Statistical analysis of the data was performed with GraphPad PRISM (GraphPad Software, Inc,
160 USA). Data is always shown as mean \pm SEM. A detailed overview of all averaged data can be
161 found in supplementary data tables S3-S7. Mann-Whitney U test, unpaired Student's T test or
162 one-way ANOVA with Dunnet's correction for multiple-comparisons was used for statistical
163 analysis. P<0.05 was considered significant.

164 **Results**

165 **Generation of DA neurons derived from individuals with and without Brunner syndrome**

166 We generated hiPSCs from two healthy subjects and three Brunner syndrome patients from
167 independent families (**Figure 1a**, for extended information see **Supplementary Table S1**).
168 ME2 and ME8 had a missense mutation in exon 2 (c.133C>T, p.R45W(8)) and exon 8
169 (c.797_798delinsTT, p.C266F(7)), respectively. These mutations are both located in the flavin
170 adenine dinucleotide (FAD)-binding domain of MAOA(8) (**Figure 1b**). NE8 had a nonsense
171 mutation in *MAOA* leading to a premature stop codon (c.886C>T, p.Q296**)(5). All patients
172 were known to display elevated serotonin and disturbed monoamine metabolite levels in serum
173 and urine(3, 6-8). All selected clones expressed the pluripotency markers OCT4, TRA-1-81,
174 NANOG, and SSEA4 (**Supplementary Figure 1**), and *MAOA* mutations were confirmed by
175 Sanger sequencing in the fibroblast-derived hiPSC lines from individuals with Brunner
176 syndrome (**Figure 1a**).

177 We differentiated hiPSCs into a homogenous population of DA neurons using small
178 molecules(31) (**Figure 1c**). For all experiments, DA neurons were co-cultured with rodent
179 astrocytes to facilitate neuronal development and network maturation. Neuronal identity was
180 confirmed by microtubule-associated protein 2 (MAP2) expression and DA neuron identity by
181 expression of the dopaminergic neuron marker tyrosine hydroxylase (TH) after 55 days *in vitro*
182 (DIV 55, **Figure 1d**). All hiPSC lines were able to differentiate into TH/MAP2 double-positive
183 neurons at similar efficiency (**Figure 1e**).(31)*MAOA* mRNA levels were similar between
184 control lines (**Figure 1f**), and the ME2 and ME8 lines (**Figure 1g**). As expected, mRNA levels
185 of *MAOA* were reduced in the NE8 line compared to healthy controls (**Figure 1g**). This is likely
186 caused by nonsense-mediated mRNA decay, which has been reported in human fibroblasts

187 with the same mutation(35). Of note, ME2 and NE8 carry an allele of the variable number
188 tandem repeat (VNTR) polymorphism in the MAOA promoter region associated with high
189 gene expression (36, 37), whereas control-1, control-2 and ME8 carry an allele associated with
190 low expression (**Supplementary Figure 2**). These alleles have previously been suggested to
191 affect *MAOA* expression differentially using luciferase assays in immortalized cell lines(38).
192 However, in hiPSC-derived DA neurons, *MAOA* expression does not seem to be affected by
193 this polymorphism.

194

195 **MAOA dysfunction affects synapse density in DA neurons**

196 It has been shown that dendritic arborization of pyramidal neurons in the orbitofrontal cortex
197 is increased in *Maoa* hemizygous knockout mice(17). However, it is unclear whether this is a
198 direct effect of impaired MAOA expression or function. We therefore immunostained MAP2
199 to identify the soma and dendrites of DA neurons (**Supplementary Figure 3**) and used
200 quantitative morphometric analysis to assess whether MAOA dysfunction directly affects
201 neuronal somatodendritic morphology (**Figure 2a**). Comparison of DA neurons from healthy
202 individuals and those with Brunner syndrome revealed cell-line specific alterations of DA
203 neuron morphology after 73 days of differentiation (DIV 73). ME8 DA neurons showed a
204 significant increase in soma size (**Figure 2b**) and dendrite complexity including dendritic
205 nodes, length and Sholl analysis (**Figure 2c, d, f**, respectively) compared to controls. Whilst
206 NE8 DA neurons showed no differences from controls in dendritic complexity (**Figure 2c-f**).
207 Both ME8 and ME2 DA neurons showed a significant increase in the total dendritic span
208 (Convex Hull analysis, **Figure 2g**), which suggests that missense mutations in the FAD of
209 *MAOA* similarly affect MAOA function.

210 In addition to alterations in dendritic complexity(39, 40), neurodevelopmental disorders have
211 been associated with synaptic deficits in rodents and humans(41). We therefore estimated
212 synapse density using the number of presynaptic synapsin1/2 puncta per section of postsynaptic
213 dendrite. We found that synapse density was significantly decreased in DA neurons from all
214 three Brunner syndrome-derived lines compared to DA neurons from healthy controls at
215 DIV73 (**Figure 2h, i**). This suggests that, whilst the effect of MAOA dysfunction on DA
216 neuron morphology might be mutation- and/or patient specific, MAOA dysfunction induced
217 reduction of synapse density is a general feature of DA neurons in Brunner syndrome.

218 **Brunner syndrome-derived DA neurons show increased neuronal network activity**

219 Differences in network activity and organization have been observed in the brain of individuals
220 with neurodevelopmental disorders(42), and changes in synapse density have been shown to
221 underlie these neuronal network changes(40, 43). To investigate the neuronal network
222 phenotypes by means of recording extracellular spontaneous activity at the population level,
223 we generated control and Brunner syndrome DA neuron cultures grown on 6-well MEAs
224 (**Figure 3a**). We recorded the network activity at DIV 73, the same *in vitro* timepoint at which
225 the reduced synapse density was observed, and compared control DA neuron networks with
226 patient networks. At this timepoint, neuronal cultures generated spontaneous activity (**Figure**
227 **3b-d**), and control lines showed similar, albeit sparse, activity levels (control-1 and control-2,
228 **Supplementary Figure 4**). Since we detected no difference in neuronal activity between the
229 ME2 and ME8 lines, and our data on synapse density suggest that dysfunction of the FAD
230 domain similarly affects MAOA function in these lines (**Supplementary Figure 4**), we
231 grouped data from the missense mutation lines for statistical analysis. Control networks mainly
232 showed sporadic random spiking activity (**Figure 3b, e**), whereas synchronous activity at either

233 the single electrode level (burst activity, **Figure 3f**) or throughout the entire culture (network
234 burst activity, **Figure 3g**) was largely absent. By contrast, Brunner syndrome DA neuronal
235 networks showed significantly higher random spiking activity at DIV 73 compared to control
236 (**Figure 3e**). Moreover, in Brunner syndrome networks, activity occurred organized into
237 readily observable synchronous events (network bursts) composed of many spikes occurring
238 close in time and across the culture (**Figure 3b-c, g**). This indicates that Brunner syndrome DA
239 neurons are more strongly integrated into a spontaneously active network than control neurons
240 at DIV 73.

241 **MAOA dysfunction does not affect intrinsic properties and AMPAR-mediated synaptic** 242 **transmission**

243 We hypothesized that the increased network activity in Brunner syndrome DA neurons might
244 be caused by changes in intrinsic properties of our DA neurons. We used whole-cell patch
245 clamp to investigate passive and active intrinsic membrane properties of DA neurons, which
246 are a measure of neuronal development and neuronal health(44). All DA neurons generated
247 action potentials upon positive current injection to the cell soma (**Figure 4a**). At DIV 73,
248 membrane capacitance, membrane resistance and membrane resting membrane potential were
249 comparable across all cell lines, indicating that all assessed DA neurons showed comparable
250 ion channel expression and level of maturity (**Figure 4b-d**). Furthermore, active (related to the
251 action potential) properties were comparable between control and patient neurons as well
252 (**Figure 4e-g**). These data suggest that the cell autonomous excitability and the intrinsic
253 properties of DA neurons are not affected by mutation of *MAOA*.

254 (45-47). The reduced synapse density in all Brunner syndrome DA neuron lines and the
255 increased network activity on the MEA suggest that synaptic transmission might be affected

256 by MAOA dysfunction. Therefore, we explored whether α -amino-3-hydroxy-5-methyl-4-
257 isoxazolepropionic acid receptor (AMPA)-mediated spontaneous excitatory postsynaptic
258 currents (sEPSCs) are altered in DIV 73 Brunner syndrome DA neurons. Neither sEPSC
259 frequency nor amplitude were affected between control and Brunner syndrome DA neurons
260 (**Figure 4h-j**). Consistent with this, we did not find a significant change in mRNA expression
261 of the most common AMPAR subunits (*GRIA1-4*) across lines (**Supplementary Figure 5**).
262 We did observe an increase in mRNA expression of the *GRIA1* subunit in the NE8 line, but
263 this was not reflected by a change in AMPAR-mediated currents. Taken together, these data
264 show that AMPAR-mediated currents are not affected by MAOA dysfunction.

265 **MAOA dysfunction leads to NMDAR hyperfunction**

266 Next to AMPAR mediated currents, NMDAR-mediated currents are an important component
267 of balanced network activity both *in vitro* and *in vivo*, and changes in NMDAR function have
268 been shown to affect network function in hiPSC-derived neuronal cultures(33, 48). We
269 therefore hypothesized that aberrant NMDAR function could be responsible for the hyperactive
270 network phenotypes in the Brunner syndrome DA neurons. To test this, we measured the
271 transcripts of the most common NMDAR subunits by RT-qPCR for all hiPSC derived DA
272 neuron lines. We found no significant changes in *GRIN1* mRNA expression, which codes for
273 the mandatory subunit present in functional NMDARs (**Figure 4k**). However, we found a two-
274 fold upregulation of *GRIN2A* and *GRIN2B* mRNA, which encode NMDAR subunit 2A and
275 subunit 2B, respectively (**Figure 4l-m**). Aberrant expression of *GRIN2A* and *GRIN2B* has been
276 shown to directly affect NMDA mediated current responses(49, 50). To test whether the
277 increased NMDAR subunit expression leads to increased NMDAR-mediated currents, control
278 and missense Brunner syndrome DA neurons were stimulated with a local exogenous

279 application of NMDA We found that the total current transfer mediated by the NMDA
280 application was significantly increased in these neurons compared to controls (**Figure 4o-p**).
281 Taken together, this suggests that increased NMDAR expression or function might underlie
282 the increased network activity observed in Brunner syndrome DA neuronal networks at DIV
283 73.

284 **Correction of *MAOA* mutation restores NMDAR expression and DA neuronal network** 285 **activity**

286 Our data suggest that the increase in *GRIN2A* and *GRIN2B* expression in the patient lines, and
287 the concomitant increase in NMDA mediated currents in the ME2 and ME8 missense lines, are
288 a direct consequence of *MAOA* mutation. In order to further validate this causality, we
289 generated an isogenic hiPSC line (ME8-CRISPR) in which we corrected the p.C266F mutation
290 present in the ME8 line through CRISPR/Cas9 mediated homologous recombination (**Figure**
291 **5a, Supplementary Figure 6**). We found that NMDAR subunit transcript levels in ME8-
292 CRISPR DA neurons were similar to control values at DIV 73 (**Figure 5b-d**). This further
293 indicates that normal *MAOA* activity is essential for the regulation of *GRIN2A* and *GRIN2B*
294 expression. Correction of the ME8 missense mutation also resulted in the normalization of the
295 NMDA-induced NMDAR-mediated current transfer (**Figure 5e, f**). Finally, we found that
296 restoration of *MAOA* function also normalized activity on the MEA to control values (**Figure**
297 **5g**); whereas ME8 DA neurons showed increased network activity, this increase was absent in
298 ME8-CRISPR DA neuronal networks, as the mean firing rate (**Figure 5h**) and mean burst rate
299 (**Figure 5i**) were similar to control values. Therefore, we conclude that rescue of *MAOA*
300 mutation results in normalization of *GRIN2A* and *GRIN2B* expression, which is reflected by a
301 restoration of neuronal network activity to control values. This implicates aberrant expression

302 of NMDARs in the neuronal network phenotype observed in DA neurons derived from
303 individuals with Brunner syndrome.

304

305 **Discussion**

306 Monoamine aberration through dysfunction of MAOA results in Brunner syndrome. Although
307 the syndrome has been described almost three decades ago, insight into the molecular
308 mechanisms of the disorder is still lacking. Here, we developed a hiPSC-derived DA neuron
309 model to assess the molecular and cellular phenotypes underlying brain dysfunction in Brunner
310 syndrome. Until now, only four families have been reported in which individuals have Brunner
311 syndrome(5-8). We were able to include individuals from three of these families into our study.
312 hiPSC-derived DA neurons generated from individuals with Brunner syndrome showed
313 reduced synapse density but increased network activity. The phenotype could be linked to
314 increased *GRIN2A* and *GRIN2B* expression and NMDAR hyperfunction. Lastly, we were able
315 to restore DA neuronal network activity and NMDAR-mediated activity to control values by
316 correcting a missense mutation using CRISPR/Cas9.

317 One of the opportunities of hiPSC technology is that patient-specific mutations can be
318 investigated using patient-derived cell lines. In our case, we found that lines from the different
319 individuals with Brunner syndrome exhibit both overlapping and distinct phenotypes. As such,
320 some differences between control and patient-derived DA neurons could not be reliably
321 attributed to MAOA dysfunction. For example, DA neuron dendritic morphology between
322 lines derived from individuals with and without Brunner syndrome was highly cell line
323 specific, and we suspect that the differences we found between control and Brunner syndrome
324 lines were strongly affected by the individual genetic background rather than being a clear

325 consequence of MAOA dysfunction. This contrasts with conclusions drawn from previous
326 studies of hemizygous *Maoa* knockout mice, in which increased dendritic arborization of
327 pyramidal neurons in the orbitofrontal cortex was described(51). However, it is not known
328 whether affected neurons in mouse orbitofrontal cortex expressed MAOA. As such, the
329 changes in neuronal morphology in these mice do not necessarily reflect an effect of cell
330 autonomous reduction of MAOA expression. Instead, it is possible that differences in
331 monoamine levels in these mice during brain development can affect neuronal morphology, as
332 monoamines such as dopamine and serotonin can induce neurite growth in rodent neurons(13,
333 52, 53). Additionally, our human DA neuron cultures are dependent on glial support from
334 wildtype rodent astrocytes, which express both MAOA and MAOB(54) and are highly
335 involved in the maintenance of dopamine levels *in vivo*(38). As such, the influence of MAOA
336 dysfunction in the human DA neurons on extracellular dopamine levels in our *in vitro* cultures
337 might be limited, which could lead to occlusion of somatodendritic phenotypes. Recent
338 developments that enable the generation of homogenous cultures of hiPSC derived
339 astrocytes(55) offer exciting opportunities to further explore the contribution of non-neuronal
340 MAOA dysfunction to monoamine aberration *in vitro*.

341 Recent single cell RNAseq profiling confirms that *MAOA* is not exclusively expressed in DA
342 neurons, but is expressed in neural progenitor cells and other monoaminergic neurons(26, 56).
343 Similar to aberrant dopamine signaling, dysfunction of serotonergic systems is associated with
344 aggression and impulsivity(23, 57). We constrained our investigation to MAOA dysfunction
345 in a homogenous DA neuron population, where MAOA dysfunction shows a clear neuronal
346 phenotype. It will be interesting to extend these investigations to include other monoaminergic
347 neuron types, and established protocols to generate a homogenous population of hiPSC-derived

348 serotonergic neurons(37, 58). Thus, it is possible to assess whether the same molecular
349 mechanisms affected by MAOA dysfunction in DA neurons can be generalized to other neuron
350 subtypes in which MAOA is expressed.

351 The individuals with Brunner syndrome all carry rare mutations, which lead to either complete
352 loss or reduced activity of the MAOA enzyme (5-7, 35). In the general population, the VNTR
353 polymorphism in the promoter of *MAOA* can induce different levels of transcriptional
354 activity(36). Low activity alleles of *MAOA* (*MAOA-L*) has been associated with increased anti-
355 social behavior in individuals subjected to childhood maltreatment(59, 60). Interestingly, we
356 recently showed increased structural and functional connectivity of brain regions associated
357 with emotion regulation in healthy individuals carrying *MAOA-L* alleles compared to those
358 carrying high activity *MAOA* (*MAOA-H*) alleles using magnetic resonance imaging(61). The
359 individuals with Brunner syndrome included here carry both *MAOA-L* (ME8) and *MAOA-H*
360 (ME2 and NE8). Intriguingly, the ME8 DA neurons did show an increase in dendritic
361 complexity compared to both controls and the ME2 and NE8 patient lines. However, this did
362 not result in differences in the functional network phenotype between ME8 and the other lines.
363 Furthermore, ME2, ME8 and NE8 all showed similar synapse densities and *GRIN2A* and
364 *GRIN2B* expression. This suggests that not all functional phenotypes shown by MAOA
365 dysfunction are affected by the presence of *MAOA-L* or *MAOA-H* VNTRs. The increased
366 dendritic complexity might be a consequence of MAOA dysfunction aggravated by the
367 presence of the *MAOA-L* VNTR. Further exploration of how low and high activity *MAOA*
368 alleles affect DA neuron function in healthy subjects can help us understand molecular
369 mechanisms regulated by MAOA.

370 Similar to the effect of MAOA dysfunction in human DA neurons, increased expression of the
371 *GRIN2A* and *GRIN2B* NMDAR subunits has been observed in prefrontal cortex of *Maoa*
372 hemizygous knockout mice. The prefrontal cortex is a highly heterogenous region, and until
373 now it was unclear whether the changes in NMDAR expression and NMDA mediated currents
374 that were observed in *Maoa* hemizygous knockout mouse were established through cell-
375 autonomous mechanisms. Isogenic rescue of MAOA mutation in the ME8 line results in
376 normalization of *GRIN2A* and *GRIN2B* expression and NMDAR-mediated currents to control
377 levels, which suggests that MAOA dysfunction cell-autonomously affects NMDAR activity.
378 Importantly, the restoration of NMDAR function results in reversal of the network phenotype
379 in DA neuron cultures, which could also be an explanation for the positive effects of NMDAR
380 antagonism on locomotor behavior of *Maoa* hemizygous knockout mice(19). The overlap in
381 mechanisms affected in the prefrontal cortex of these mice and hiPSC-derived DA neurons of
382 individuals with Brunner syndrome shows that DA neuron cultures are a viable *in vitro* system
383 to investigate possible therapeutic strategies.

384 The protocol we describe here results in highly homogenous and reproducible cultures of DA
385 neurons. Growing hiPSC-derived DA neuron networks on MEAs enables us to study patient-
386 specific neuronal networks. Most investigations that use hiPSC-derived DA neurons have
387 focused on cell-based therapy for neurodegenerative disorders such as Parkinson's disease,
388 lacking characterization of network activity(62, 63). In one study, hiPSC derived DA neurons
389 have been cultured on MEAs to investigate neuronal phenotypes in a monozygotic twin pair
390 discordant for Parkinson's disease(64). Reduced network activity was seen in DA neurons
391 derived from the twin with Parkinson's disease, which shows that network phenotypes of
392 hiPSC derived DA neurons can be characterized using MEAs. In our study, we combine an

393 extensive characterization of both the single-cell and network properties of hiPSC-derived DA
394 neurons and how these can be related to differences at the molecular level in
395 neurodevelopmental disorders with a monogenic cause.

396 In conclusion, our data suggest that MAOA dysfunction affects DA neuron function in
397 individuals with Brunner syndrome and that NMDAR hyperfunction is a key contributor to
398 network dysfunction in Brunner syndrome DA neuron cultures. These alterations on the
399 network level might be able to explain parts of Brunner syndrome associated impulsivity and
400 maladaptive externalizing behavior. Manipulation of NMDAR function could be a viable
401 opportunity toward the development of possible therapeutic strategies.

402

403 **Acknowledgements**

404 The authors would like to acknowledge support from the Netherlands Organization for
405 Scientific Research (NWO) Vici Innovation Program (grant 016-130-669 to BF), from the
406 European Community's Seventh Framework Programme (FP7/2007–2013) under grant
407 agreement no. 602805 (Aggressotype), and from the European Community's Horizon 2020
408 Programme (H2020/2014–2020) under grant agreements no. 667302 (CoCA) and no. 728018
409 (Eat2beNICE). Additional support is received from the Dutch National Science Agenda for the
410 NeurolabNL project (grant 40017602) the NWO grant 012.200.001 and 91217055 (to N.N.K.),
411 SFARI grant 610264 (to N.N.K), ERA-NET NEURON DECODE! grant (NWO) 013.18.001
412 (to N.N.K) and ERA-NET NEURON-102 SYNSCHIZ grant (NWO) 013-17-003.4538 (to
413 D.S).

414 **Author contributions**

415 Y.S., J.v.R., B.F. and N.N.K. conceived and supervised the study. Y.S., J.v.R., B.F. and N.N.K.
416 designed all the experiments. Y.S. performed all cell culture, generated the isogenic
417 CRISPR/Cas9 mediated lines and acquired all MEA data. J.v.R. performed all single-cell
418 electrophysiological experiments, M.B. performed neuronal reconstruction. B.M., M.H.,
419 T.K.G., C.S. performed additional experiments. M.F., S.K-S, D.S., H.B., L.F. and E.P.
420 provided resources. Y.S., J.v.R., M.B., B.M. performed data analysis. Y.S., J.v.R., B.F., and
421 N.N.K. wrote the paper. D.S., H.B., and B.F. edited the paper.

422 **Competing interests**

423 BF has received educational speaking fees from Medice. The other authors declare to have no
424 competing interests.

425 References

- 426 1. Ruhe HG, Mason NS, Schene AH (2007): Mood is indirectly related to serotonin,
427 norepinephrine and dopamine levels in humans: A meta-analysis of monoamine depletion
428 studies. *Mol Psychiatr.* 12:331-359.
- 429 2. Levitt P, Harvey JA, Friedman E, Simansky K, Murphy EH (1997): New evidence for
430 neurotransmitter influences on brain development. *Trends Neurosci.* 20:269-274.
- 431 3. Godar SC, Fite PJ, McFarlin KM, Bortolato M (2016): The role of monoamine oxidase
432 A in aggression: Current translational developments and future challenges. *Prog*
433 *Neuropsychopharmacol Biol Psychiatry.* 69:90-100.
- 434 4. Bortolato M, Chen K, Shih JC (2008): Monoamine oxidase inactivation: from
435 pathophysiology to therapeutics. *Adv Drug Deliv Rev.* 60:1527-1533.
- 436 5. Brunner HG, Nelen M, Breakefield XO, Ropers HH, van Oost BA (1993): Abnormal
437 behavior associated with a point mutation in the structural gene for monoamine oxidase A.
438 *Science.* 262:578-580.
- 439 6. Brunner HG, Nelen MR, van Zandvoort P, Abeling NG, van Gennip AH, Wolters EC,
440 et al. (1993): X-linked borderline mental retardation with prominent behavioral disturbance:
441 phenotype, genetic localization, and evidence for disturbed monoamine metabolism. *Am J Hum*
442 *Genet.* 52:1032-1039.
- 443 7. Piton A, Poquet H, Redin C, Masurel A, Lauer J, Muller J, et al. (2014): 20 ans apres:
444 a second mutation in MAOA identified by targeted high-throughput sequencing in a family
445 with altered behavior and cognition. *Eur J Hum Genet.* 22:776-783.
- 446 8. Palmer EE, Leffler M, Rogers C, Shaw M, Carroll R, Earl J, et al. (2016): New insights
447 into Brunner syndrome and potential for targeted therapy. *Clinical Genetics.* 89:120-127.
- 448 9. van Erp AM, Miczek KA (2000): Aggressive behavior, increased accumbal dopamine,
449 and decreased cortical serotonin in rats. *J Neurosci.* 20:9320-9325.
- 450 10. Ferrari PF, van Erp AM, Tornatzky W, Miczek KA (2003): Accumbal dopamine and
451 serotonin in anticipation of the next aggressive episode in rats. *Eur J Neurosci.* 17:371-378.
- 452 11. Alekseyenko OV, Chan YB, Li R, Kravitz EA (2013): Single dopaminergic neurons
453 that modulate aggression in Drosophila. *Proceedings of the National Academy of Sciences of*
454 *the United States of America.* 110:6151-6156.
- 455 12. Couppis MH, Kennedy CH (2008): The rewarding effect of aggression is reduced by
456 nucleus accumbens dopamine receptor antagonism in mice. *Psychopharmacology.* 197:449-
457 456.
- 458 13. Money KM, Stanwood GD (2013): Developmental origins of brain disorders: roles for
459 dopamine. *Front Cell Neurosci.* 7:260.
- 460 14. Rodriguiz RM, Chu R, Caron MG, Wetsel WC (2004): Aberrant responses in social
461 interaction of dopamine transporter knockout mice. *Behav Brain Res.* 148:185-198.
- 462 15. Cases O, Seif I, Grimsby J, Gaspar P, Chen K, Pournin S, et al. (1995): Aggressive
463 behavior and altered amounts of brain serotonin and norepinephrine in mice lacking MAOA.
464 *Science.* 268:1763-1766.
- 465 16. Scott AL, Bortolato M, Chen K, Shih JC (2008): Novel monoamine oxidase A knock
466 out mice with human-like spontaneous mutation. *NeuroReport.* 19:739-743.

- 467 17. Bortolato M, Chen K, Godar SC, Chen G, Wu W, Rebrin I, et al. (2011): Social Deficits
468 and Perseverative Behaviors, but not Overt Aggression, in MAO-A Hypomorphic Mice.
469 *Neuropsychopharmacology*. 36:2674-2688.
- 470 18. Cases O, Vitalis T, Seif I, De Maeyer E, Sotelo C, Gaspar P (1996): Lack of barrels in
471 the somatosensory cortex of monoamine oxidase A-deficient mice: role of a serotonin excess
472 during the critical period. *Neuron*. 16:297-307.
- 473 19. Bortolato M, Godar SC, Melis M, Soggiu A, Roncada P, Casu A, et al. (2012):
474 NMDARs Mediate the Role of Monoamine Oxidase A in Pathological Aggression. *Journal of*
475 *Neuroscience*. 32:8574-8582.
- 476 20. Luque JM, Kwan SW, Abell CW, Da Prada M, Richards JG (1995): Cellular expression
477 of mRNAs encoding monoamine oxidases A and B in the rat central nervous system. *J Comp*
478 *Neurol*. 363:665-680.
- 479 21. Bortolato M, Floris G, Shih JC (2018): From aggression to autism: new perspectives on
480 the behavioral sequelae of monoamine oxidase deficiency. *J Neural Transm (Vienna)*.
- 481 22. Evrard A, Malagie I, Laporte AM, Boni C, Hanoun N, Trillat AC, et al. (2002): Altered
482 regulation of the 5-HT system in the brain of MAO-A knock-out mice. *Eur J Neurosci*. 15:841-
483 851.
- 484 23. Seo D, Patrick CJ, Kennealy PJ (2008): Role of Serotonin and Dopamine System
485 Interactions in the Neurobiology of Impulsive Aggression and its Comorbidity with other
486 Clinical Disorders. *Aggress Violent Behav*. 13:383-395.
- 487 24. Nagatsu T (2004): Progress in monoamine oxidase (MAO) research in relation to
488 genetic engineering. *Neurotoxicology*. 25:11-20.
- 489 25. Vitalis T, Fouquet C, Alvarez C, Seif I, Price D, Gaspar P, et al. (2002): Developmental
490 expression of monoamine oxidases A and B in the central and peripheral nervous systems of
491 the mouse. *J Comp Neurol*. 442:331-347.
- 492 26. La Manno G, Gyllborg D, Codeluppi S, Nishimura K, Salto C, Zeisel A, et al. (2016):
493 Molecular Diversity of Midbrain Development in Mouse, Human, and Stem Cells. *Cell*.
494 167:566-580 e519.
- 495 27. Pinto D, Delaby E, Merico D, Barbosa M, Merikangas A, Klei L, et al. (2014):
496 Convergence of genes and cellular pathways dysregulated in autism spectrum disorders. *Am J*
497 *Hum Genet*. 94:677-694.
- 498 28. de Almeida RM, Ferrari PF, Parmigiani S, Miczek KA (2005): Escalated aggressive
499 behavior: dopamine, serotonin and GABA. *Eur J Pharmacol*. 526:51-64.
- 500 29. Soares E, Xu Q, Li Q, Qu J, Zheng Y, Raeven HHM, et al. (2019): Single-cell RNA-
501 seq identifies a reversible mesodermal activation in abnormally specified epithelia of p63 EEC
502 syndrome. *Proceedings of the National Academy of Sciences*.201908180.
- 503 30. Mandegar MA, Huebsch N, Frolov EB, Shin E, Truong A, Olvera MP, et al. (2016):
504 CRISPR Interference Efficiently Induces Specific and Reversible Gene Silencing in Human
505 iPSCs. *Cell Stem Cell*. 18:541-553.
- 506 31. Sundberg M, Bogetofte H, Lawson T, Jansson J, Smith G, Astradsson A, et al. (2013):
507 Improved Cell Therapy Protocols for Parkinson's Disease Based on Differentiation Efficiency
508 and Safety of hESC-, hiPSC-, and Non-Human Primate iPSC-Derived Dopaminergic Neurons.
509 *STEM CELLS*. 31:1548-1562.
- 510 32. Frega M, van Gestel SHC, Linda K, van der Raadt J, Keller J, Van Rhijn J-R, et al.
511 (2017): Rapid Neuronal Differentiation of Induced Pluripotent Stem Cells for Measuring
512 Network Activity on Micro-electrode Arrays.e54900.

- 513 33. Frega M, Linda K, Keller JM, Gumus-Akay G, Mossink B, van Rhijn JR, et al. (2019):
514 Neuronal network dysfunction in a model for Kleefstra syndrome mediated by enhanced
515 NMDAR signaling. *Nature Communications*. 10.
- 516 34. Bologna LL, Pasquale V, Garofalo M, Gandolfo M, Baljon PL, Maccione A, et al.
517 (2010): Investigating neuronal activity by SPYCODE multi-channel data analyzer. *Neural*
518 *Netw*. 23:685-697.
- 519 35. Chen K, Holschneider DP, Wu WH, Rebrin I, Shih JC (2004): A spontaneous point
520 mutation produces monoamine oxidase A/B knock-out mice with greatly elevated monoamines
521 and anxiety-like behavior. *Journal of Biological Chemistry*. 279:39645-39652.
- 522 36. Sabol SZ, Hu S, Hamer D (1998): A functional polymorphism in the monoamine
523 oxidase A gene promoter. *Human Genetics*. 103:273-279.
- 524 37. Vadodaria KC, Ji Y, Skime M, Paquola AC, Nelson T, Hall-Flavin D, et al. (2019):
525 Altered serotonergic circuitry in SSRI-resistant major depressive disorder patient-derived
526 neurons. *Molecular psychiatry*. 24:808-818.
- 527 38. Petrelli F, Dallerac G, Pucci L, Cali C, Zehnder T, Sultan S, et al. (2020): Dysfunction
528 of homeostatic control of dopamine by astrocytes in the developing prefrontal cortex leads to
529 cognitive impairments. *Mol Psychiatry*. 25:732-749.
- 530 39. Rivero O, Selten MM, Sich S, Popp S, Bacmeister L, Amendola E, et al. (2015):
531 Cadherin-13, a risk gene for ADHD and comorbid disorders, impacts GABAergic function in
532 hippocampus and cognition. *Transl Psychiatry*. 5:e655.
- 533 40. Chailangkarn T, Trujillo CA, Freitas BC, Hrvoj-Mihic B, Herai RH, Yu DX, et al.
534 (2016): A human neurodevelopmental model for Williams syndrome. *Nature*. 536:338-343.
- 535 41. Zoghbi HY, Bear MF (2012): Synaptic Dysfunction in Neurodevelopmental Disorders
536 Associated with Autism and Intellectual Disabilities. *Cold Spring Harbor Perspectives in*
537 *Biology*. 4.
- 538 42. Uhhaas PJ, Singer W (2006): Neural synchrony in brain disorders: Relevance for
539 cognitive dysfunctions and pathophysiology. *Neuron*. 52:155-168.
- 540 43. Marchetto MC, Belinson H, Tian Y, Freitas BC, Fu C, Vadodaria K, et al. (2017):
541 Altered proliferation and networks in neural cells derived from idiopathic autistic individuals.
542 *Mol Psychiatry*. 22:820-835.
- 543 44. Chambers SM, Qi Y, Mica Y, Lee G, Zhang XJ, Niu L, et al. (2012): Combined small-
544 molecule inhibition accelerates developmental timing and converts human pluripotent stem
545 cells into nociceptors. *Nat Biotechnol*. 30:715-720.
- 546 45. Adrover MF, Shin JH, Alvarez VA (2014): Glutamate and dopamine transmission from
547 midbrain dopamine neurons share similar release properties but are differentially affected by
548 cocaine. *J Neurosci*. 34:3183-3192.
- 549 46. Perez-Lopez JL, Contreras-Lopez R, Ramirez-Jarquín JO, Tecuapetla F (2018): Direct
550 Glutamatergic Signaling From Midbrain Dopaminergic Neurons Onto Pyramidal Prefrontal
551 Cortex Neurons. *Front Neural Circuits*. 12:70.
- 552 47. Meltzer LT, Christoffersen CL, Serpa KA (1997): Modulation of dopamine neuronal
553 activity by glutamate receptor subtypes. *Neurosci Biobehav Rev*. 21:511-518.
- 554 48. Frega M, Selten M, Mossink B, Keller JM, Linda K, Moerschen R, et al. (2020):
555 Distinct Pathogenic Genes Causing Intellectual Disability and Autism Exhibit a Common
556 Neuronal Network Hyperactivity Phenotype. *Cell Rep*. 30:173-+.

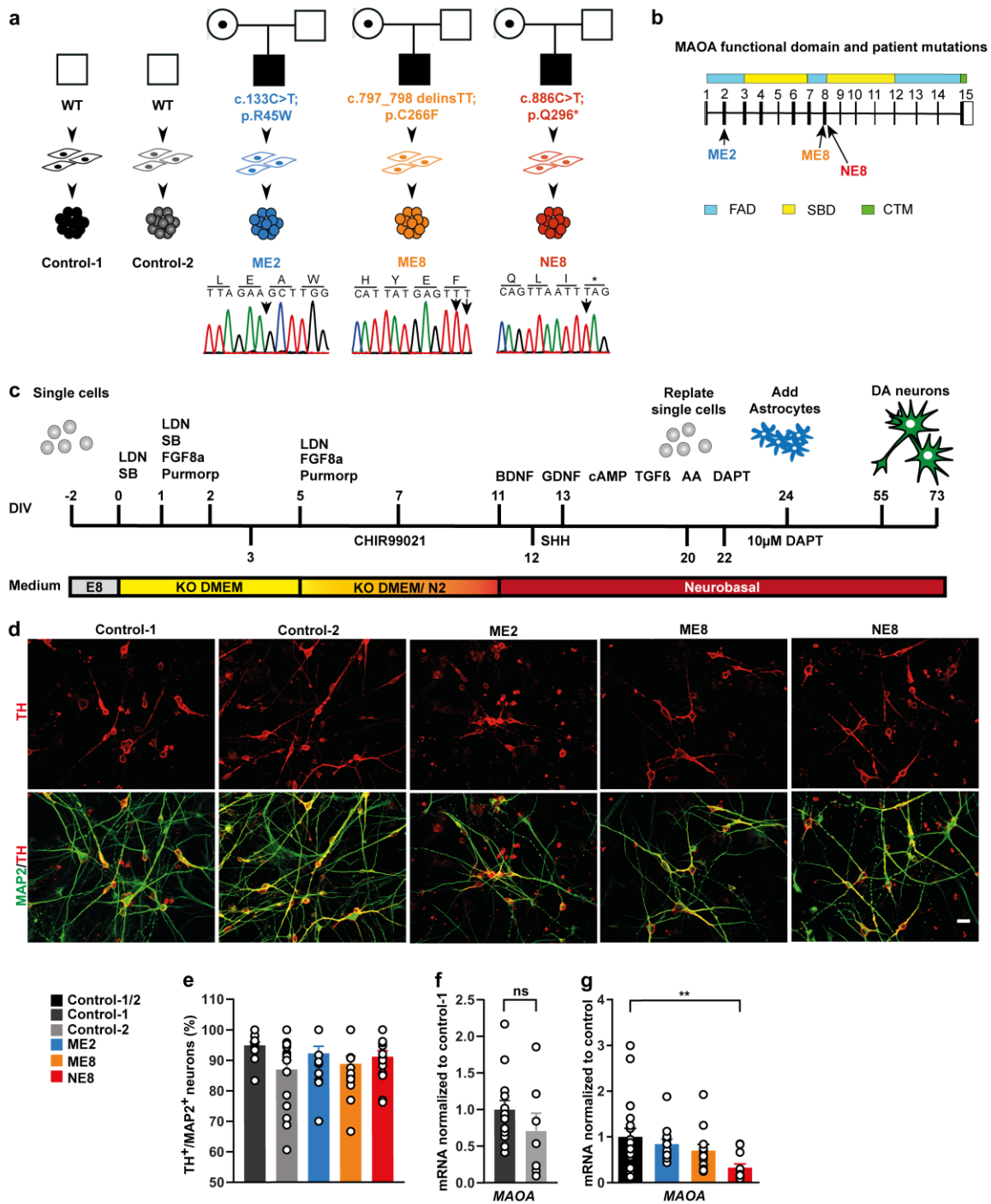
- 557 49. Endele S, Rosenberger G, Geider K, Popp B, Tamer C, Stefanova I, et al. (2010):
558 Mutations in GRIN2A and GRIN2B encoding regulatory subunits of NMDA receptors cause
559 variable neurodevelopmental phenotypes. *Nat Genet.* 42:1021-1026.
- 560 50. Myers SJ, Yuan H, Kang JQ, Tan FCK, Traynelis SF, Low CM (2019): Distinct roles
561 of GRIN2A and GRIN2B variants in neurological conditions. *F1000Res.* 8.
- 562 51. Bortolato M, Godar SC, Alzghoul L, Zhang J, Darling RD, Simpson KL, et al. (2013):
563 Monoamine oxidase A and A/B knockout mice display autistic-like features. *Int J*
564 *Neuropsychopharmacol.* 16:869-888.
- 565 52. Lotto B, Upton L, Price DJ, Gaspar P (1999): Serotonin receptor activation enhances
566 neurite outgrowth of thalamic neurones in rodents. *Neurosci Lett.* 269:87-90.
- 567 53. Schmidt U, Pilgrim C, Beyer C (1998): Differentiative effects of dopamine on striatal
568 neurons involve stimulation of the cAMP/PKA pathway. *Mol Cell Neurosci.* 11:9-18.
- 569 54. Yu PH, Hertz L (1982): Differential expression of type A and type B monoamine
570 oxidase of mouse astrocytes in primary cultures. *J Neurochem.* 39:1492-1495.
- 571 55. Nadadhur AG, Leferink PS, Holmes D, Hinz L, Cornelissen-Steijger P, Gasparotto L,
572 et al. (2018): Patterning factors during neural progenitor induction determine regional identity
573 and differentiation potential in vitro. *Stem Cell Res.* 32:25-34.
- 574 56. Södersten E, Toskas K, Rraklli V, Tiklova K, Björklund ÅK, Ringnér M, et al. (2018):
575 A comprehensive map coupling histone modifications with gene regulation in adult
576 dopaminergic and serotonergic neurons. *Nature Communications.* 9:1226.
- 577 57. Fernandez-Castillo N, Cormand B (2016): Aggressive behavior in humans: Genes and
578 pathways identified through association studies. *Am J Med Genet B Neuropsychiatr Genet.*
579 171:676-696.
- 580 58. Lu JF, Zhong XF, Liu HS, Hao L, Huang CTL, Sherafat MA, et al. (2016): Generation
581 of serotonin neurons from human pluripotent stem cells. *Nature Biotechnology.* 34:89-94.
- 582 59. Byrd AL, Manuck SB (2014): MAOA, Childhood Maltreatment, and Antisocial
583 Behavior: Meta-analysis of a Gene-Environment Interaction. *Biological Psychiatry.* 75:9-17.
- 584 60. Caspi A, McClay J, Moffitt TE, Mill J, Martin J, Craig IW, et al. (2002): Role of
585 genotype in the cycle of violence in maltreated children. *Science.* 297:851-854.
- 586 61. Harneit A, Braun U, Geiger LS, Zang ZX, Hakobjan M, van Donkelaar MMJ, et al.
587 (2019): MAOA-VNTR genotype affects structural and functional connectivity in distributed
588 brain networks. *Human Brain Mapping.* 40:5202-5212.
- 589 62. Rivetti di Val Cervo P, Romanov RA, Spigolon G, Masini D, Martin-Montanez E,
590 Toledo EM, et al. (2017): Induction of functional dopamine neurons from human astrocytes in
591 vitro and mouse astrocytes in a Parkinson's disease model. *Nat Biotechnol.* 35:444-452.
- 592 63. Kikuchi T, Morizane A, Doi D, Magotani H, Onoe H, Hayashi T, et al. (2017): Human
593 iPSC cell-derived dopaminergic neurons function in a primate Parkinson's disease model.
594 *Nature.* 548:592-596.
- 595 64. Woodard CM, Campos BA, Kuo SH, Nirenberg MJ, Nestor MW, Zimmer M, et al.
596 (2014): iPSC-derived dopamine neurons reveal differences between monozygotic twins
597 discordant for Parkinson's disease. *Cell Rep.* 9:1173-1182.

598

599

600

601 **Main Figures**

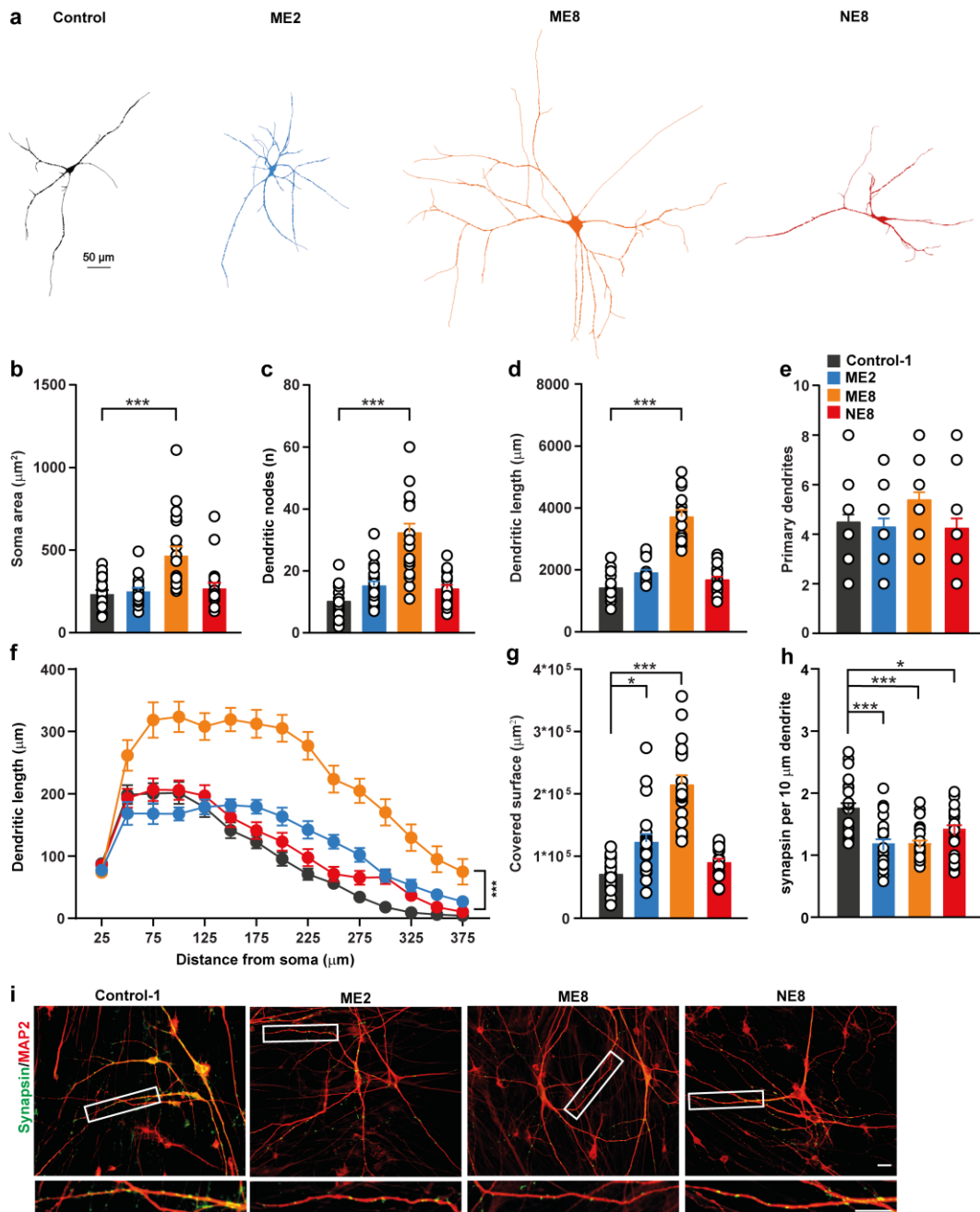


602

603 **Figure 1. Differentiation of DA neurons derived from human induced pluripotent stem**
 604 **cells (hiPSCs).** (a) Scheme of control and patient hiPSC lines used in the study. The

605 monoamine oxidase A (*MAOA*) mutations were confirmed by sanger sequencing. (b) Location
606 of the different mutations within the *MAOA* gene and protein domain. FAD (blue boxes), flavin
607 adenine dinucleotide binding domains; SBD (yellow boxes), substrate-binding domain; CTM
608 (green box), C-terminal membrane region. (c) Schematic overview of the protocol used to
609 generate DA neurons from hiPSCs. (d) Representative images of DIV 55 DA neurons labeled
610 by TH (red) and MAP2 (green) (Scale bar = 20 μ m). (e) The percentage of TH-positive neurons
611 (among MAP2-positive cells) at DIV 55. Sample size: Control-1 N=15, Control-2 N=16, ME2
612 N=15, ME8 N=15, NE8 N=15. (f) *MAOA* mRNA expression in control DIV 73 DA neurons.
613 Sample size: Control-1 N=13, Control 2 N=7. (g) Comparison of *MAOA* mRNA expression
614 between control and patient lines (Control vs NE8 $P=0.0076$). Sample size: ME2 N=12, ME8
615 N=12, NE8 N=12. All data represent means \pm SEM. One-Way ANOVA with Dunnett's
616 correction for multiple testing was used to compare between patient lines and control lines.
617 $**P<0.01$.

618



619

620 **Figure 2. Morphological organization and synapse density of DA neurons (a)**

621 Representative images of reconstructed DA neurons at 73 days of differentiation (DIV 73). (b-

622 g) Parameters derived from the somatodendritic compartment. Sample size: N=20 for all lines

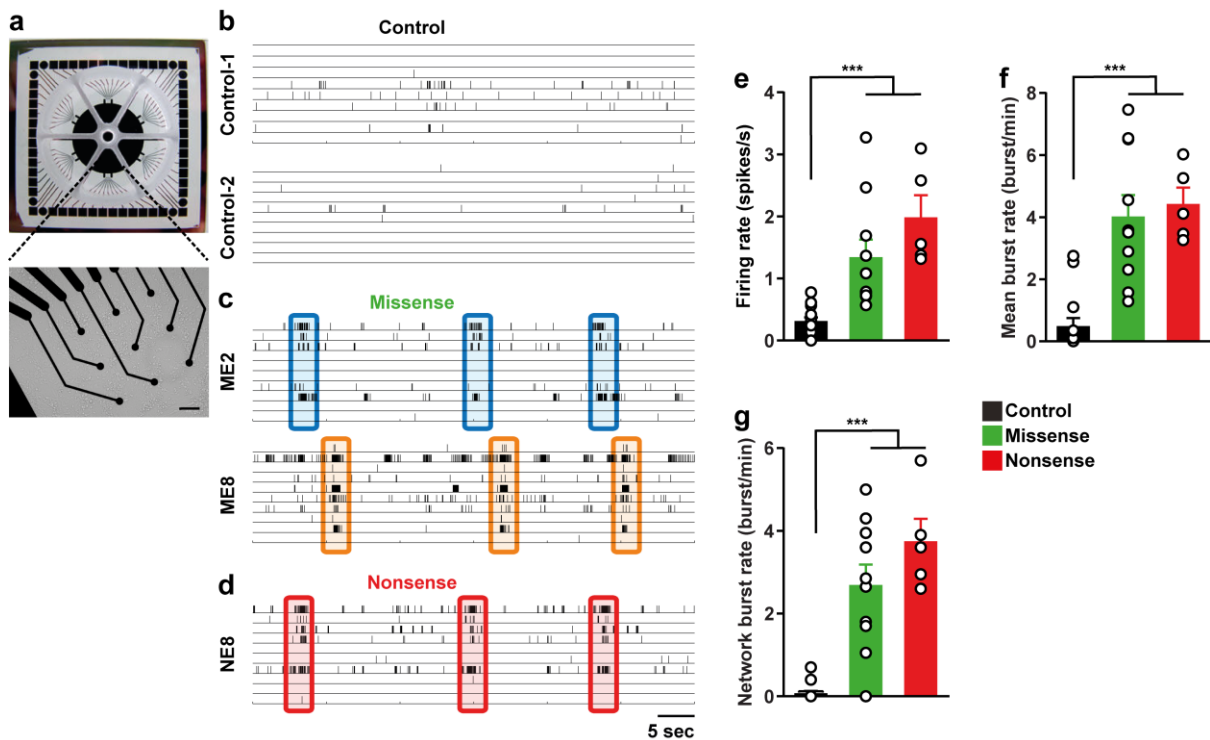
623 across 3 independent differentiations). (h) Quantifications of synapse density (N positive

624 synapsin puncta/10 μm , Sample size: Control-1 N=25, ME2 N=23, ME8 N=25, NE8 N=26. (i)

625 Representative images of control and patient DA neurons at DIV 73 immunostained for
626 microtubule associated protein 2 (MAP2) (red) and synapsin1/2 (green), scale bar = 20 μ m.
627 Inset shows a single stretch of dendrite (red) with synapses (green), scale bar = 10 μ m. All data
628 is represented as mean \pm SEM. One-Way ANOVA with Dunnett's correction for multiple
629 testing was used to compare between patient lines and control lines in all parameters except
630 Sholl analysis, where MANOVA with Bonferroni correction was used with distance and
631 genotype as factors. * $P < 0.05$; *** $P < 0.001$.

632

633



634

635 **Figure 3. Increased neuronal network activity in Brunner syndrome DA neurons.** (a)

636 Example picture of a 6-well MEA. Each chamber is fitted with 9 recording electrodes and

637 separated by a silicon nonconductive wall. (b-d) 60 second example raster plots of spontaneous

638 electrophysiological activity on MEAs with DA neuron cultures at 73 days of differentiation

639 from either healthy controls (b), or individuals with a monoamine oxidase A (*MAOA*) missense

640 mutation (c) or nonsense mutation (d). Detected spikes are indicated as black bars. Network

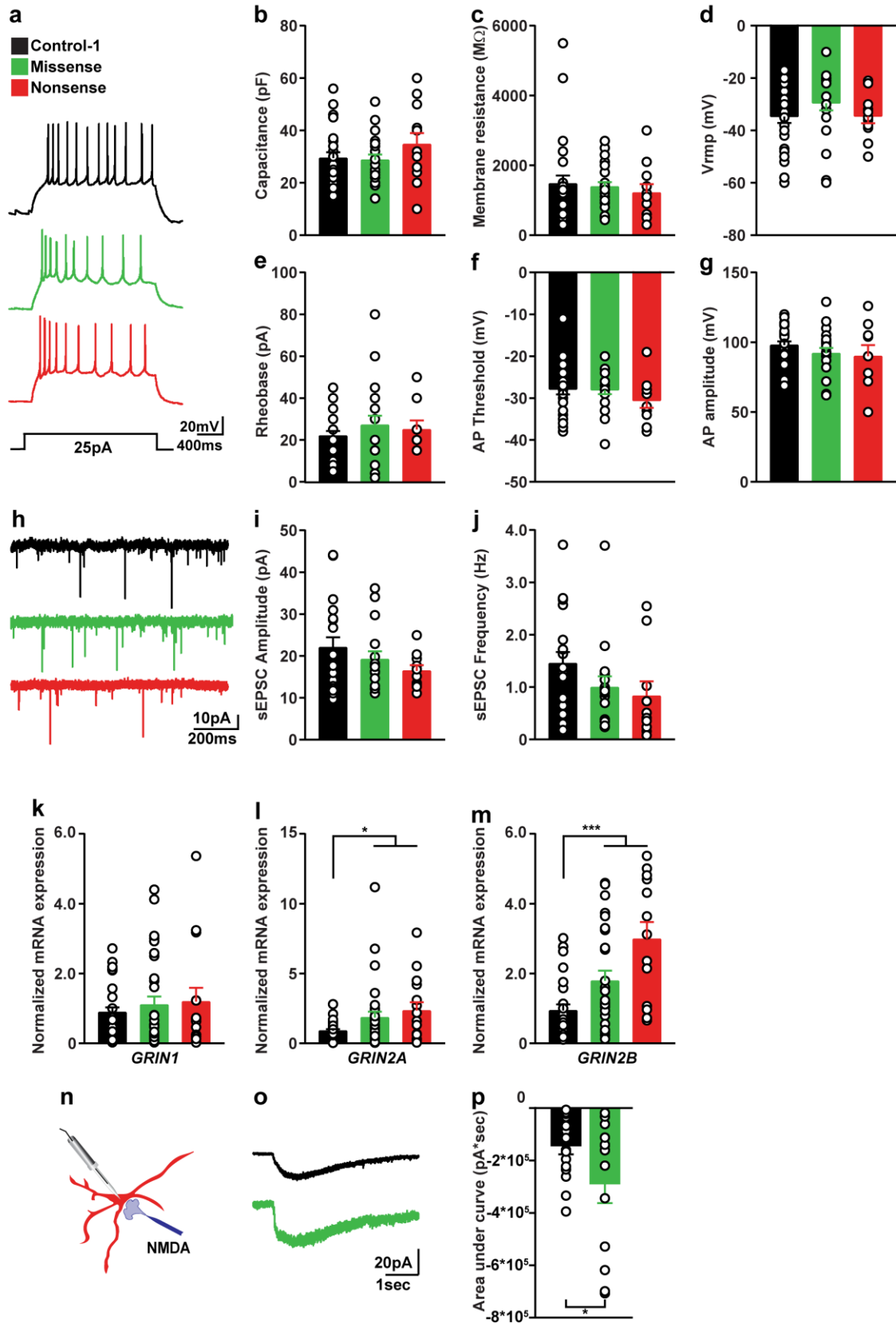
641 wide bursting activity is highlighted by colored boxes. (e) Quantification of mean firing rate.

642 (f) Quantification of mean burst rate (g) Quantification of network burst rate. Sample size:

643 control N=14, missense N=10, nonsense N=5. All data represent means \pm SEM. One-Way

644 ANOVA with Dunnett's correction for multiple testing was used to compare between patient

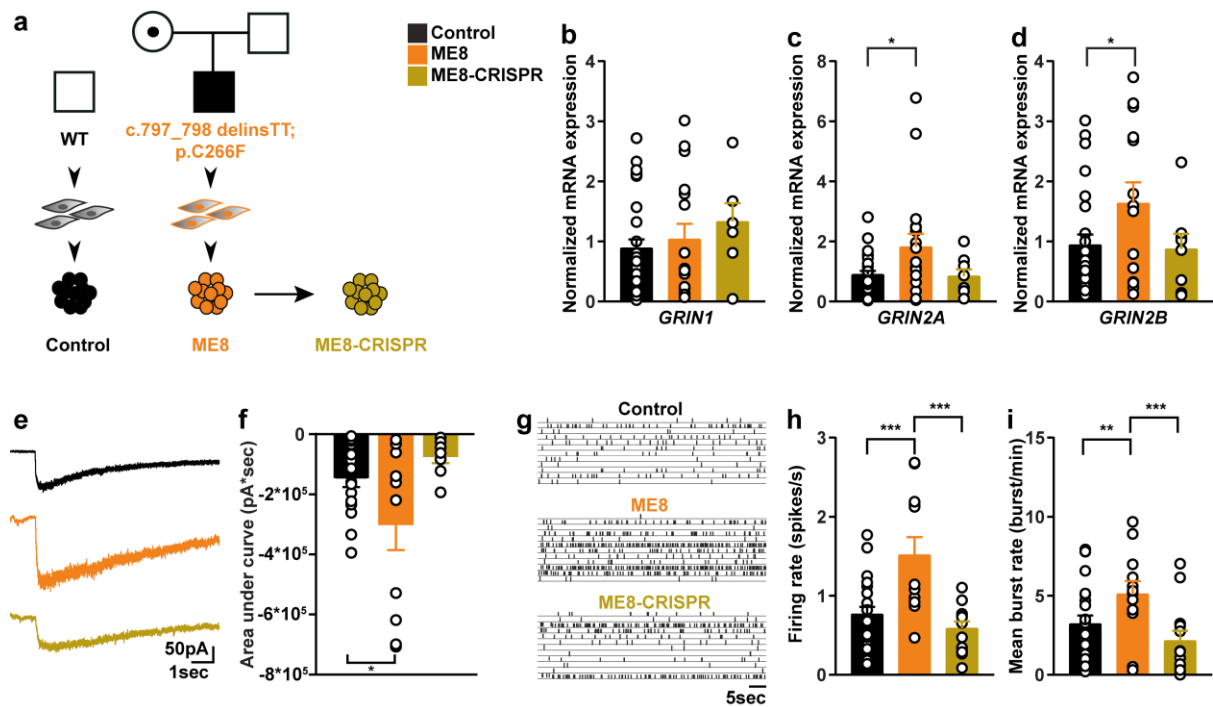
645 lines and control lines. *** $p < 0.001$.



646

647 **Figure 4. Monoamine oxidase A dysfunction results in increased N-Methyl-D-Aspartate**
648 **(NMDA) mediated excitatory currents.** (a) Representative traces of action potentials
649 generated in control and patient-derived DA neurons at 73 days of differentiation. (b-d)
650 Quantifications of passive intrinsic properties in control and patient DA neurons. (e-g)
651 Quantifications of active intrinsic properties in control and patient DA neurons at. Sample size:
652 control N=27, missense N=21, nonsense N=12. (h) Representative traces of spontaneous
653 excitatory postsynaptic current (sEPSC) activity in control- and patient-derived DA neurons at
654 DIV 73. (i,j) Quantification of spontaneous excitatory postsynaptic current (sEPSC) amplitude
655 and frequency. Sample size: control N=19, missense N=16, nonsense N=10. (k-m)
656 Quantification of mRNA expression of the NMDAR subunits NR1 (*GRIN1*), NR2A (*GRIN2A*)
657 and NR2B (*GRIN2B*). Sample size: control *GRIN1* N=32, *GRIN2A* n=29, *GRIN2B* n=25.
658 Missense *GRIN1* N=31, *GRIN2A* N=31, *GRIN2B* N=26. Nonsense *GRIN1* N=15, *GRIN2A*
659 N=15, *GRIN2B* N=13. (n) schematic representation of NMDA receptor activation experiment.
660 (o) Example traces of the current response to exogenous application of a high dose of NMDA
661 (100 ms, 10 mM) at a distance of 10-20 μm from the cell soma. (p) The area under the curve
662 (total current transfer) in control and patient lines subjected to exogenous NMDA application.
663 Sample size: control N=16, missense N=13. All data represent means \pm SEM. One-Way
664 ANOVA with Dunnett's correction for multiple testing was used to compare between control
665 and patient lines. * $P < 0.05$, *** $P < 0.001$.

666



667

668 **Figure 5. Correction of a missense mutation restores *GRIN2A* and *GRIN2B* expression,**
 669 **N-Methyl-D-Aspartate-mediated currents and neuronal network activity.** (a) Overview of
 670 the lines used for the CRISPR/Cas9-mediated rescue of Monoamine oxidase A function. (b-d)
 671 Quantification of mRNA expression of NMDAR subunits *GRIN1*, *GRIN2A* and *GRIN2B*.
 672 Sample size: control *GRIN1* N=32, *GRIN2A* N=29, *GRIN2B* N=25. ME8 *GRIN1* N=16,
 673 *GRIN2A* N=18, *GRIN2B* N=12. ME8-CRISPR *GRIN1* N=8, *GRIN2A* N=7, *GRIN2B* N=8 from
 674 at least three different neuronal preparations. (e) Example traces of the current response to
 675 exogenous NMDA application in control, ME8 and ME8-CRISPR DA neurons at 73 days of
 676 differentiation (DIV73). (f) Total current transfer (area under the curve) upon NMDA
 677 application ($P=0.0219$ between control and ME8) at DIV 73. Sample size: control N=16, ME8
 678 N=12, ME8-CRISPR N=13. (g) 60 second example trace of spontaneous network activity
 679 recorded on a 24-well microelectrode array system in control, ME8 and ME8-CRISPR DA
 680 neuronal cultures at DIV 69. (h) Quantification of mean firing rate ($P=0.00044$ between control

681 and ME8, and $P=0.00011$ between ME8 and ME8-CRISPR). (i) Quantification of mean burst
682 rate ($P=0.0048$ between control and ME8 and $P=0.0005$ between ME8 and ME8-CRISPR) at
683 DIV 69. Sample size: control N=23, patient ME-8 N=12, ME8-CRISPR N=13. One-Way
684 ANOVA with Dunnett's correction for multiple testing was used to compare control, ME8 and
685 ME8-CRISPR. Data are shown as mean \pm SEM. * $P<0.05$, ** $P<0.01$, *** $P<0.001$.